

# CNN-based LCD Transcription of Blood Pressure from a Mobile Phone Camera

Samruddhi S. Kulkarni,<sup>1,\*</sup> Nasim Katebi<sup>2,\*</sup>, Camilo E. Valderrama<sup>2</sup>, Peter Rohloff<sup>3,4</sup>, Gari D. Clifford<sup>2,5</sup>

<sup>1</sup> School of Electrical and Computer Engineering, Georgia Institute of Technology, Atlanta, GA, USA

<sup>2</sup> Department of Biomedical Informatics, Emory University, Atlanta, GA, USA

<sup>3</sup> Wuqu' Kawoq — Maya Health Alliance, Santiago Sacatepéquez, Guatemala

<sup>4</sup> Division of Global Health Equity, Brigham and Women's Hospital, Boston, MA, USA

<sup>5</sup> Department of Biomedical Engineering, Georgia Institute of Technology & Emory University, Atlanta, GA, USA

Correspondence\*:

Joint first authors:

Samruddhi S. Kulkarni, Nasim Katebi  
sskulk307@gatech.edu, nkatebi@emory.edu

## 2 ABSTRACT

3 Routine blood pressure (BP) measurement in pregnancy is commonly done using automated  
4 oscillometric devices. Since no wireless oscillometric BP device validated in preeclamptic  
5 populations exists, a simple approach to capture readings from such devices is needed, especially  
6 in low-resource settings where transmission of BP data from the field to central locations is an  
7 important mechanism for triage. A total of 8192 BP readings were captured from the Liquid Crystal  
8 Display(LCD) screen of a standard Omron M7 self-inflating BP cuff using a cellphone camera.  
9 A cohort of 49 lay midwives captured this data from 1697 pregnant women carrying singletons  
10 between 6 weeks and 40 weeks gestational age in rural Guatemala during routine screening.  
11 Images showed a wide variability in their appearance exists due to variations in orientation  
12 and parallax; environmental factors such as lighting, shadows; and image acquisition factors  
13 such as motion blur and focus problems. They were independently labelled for readability and  
14 quality by three annotators (BP range: 34 – 203 mmHg) and disagreements were resolved. The  
15 authors proposed an approach to preprocess automatically segment into diastolic BP, systolic  
16 BP and heart rate using a contour-based technique. A deep convolutional neural network was  
17 trained to convert the images of each reading into numerical values using a multi-digit recognition  
18 approach. On readable low and high quality images, the approach achieved a 91% classification  
19 accuracy and mean absolute error of 3.19 mmHg for systolic BP and 91% accuracy and mean  
20 absolute error of 0.94 mmHg for diastolic BP. These error values are within the FDA guidelines  
21 for BP monitoring when poor quality images are excluded. The proposed approach was validated  
22 by comparing against commercially available OCR tools like Tesseract and Google API The  
23 algorithm could be deployed on a phone and work without connectivity to a network.

24 **Keywords:** blood pressure, convolutional neural network, optical character recognition, digital transcription, hypertension,  
25 preeclampsia

## 1 INTRODUCTION

26 Over half a million women die each year from pregnancy-related causes, the vast majority of these deaths  
27 occur in low- and middle-income countries (LMICs) (WHO, 2005). Despite global improvements in  
28 healthcare, countries with lowest GDP per capita have made little progress and shoulder the vast majority  
29 of the global burden for fetal and maternal mortality and morbidity. There is, therefore, a critical need to  
30 focus on low-cost screening and community-based interventions to reduce preventable maternal and fetal  
31 mortality and morbidity (Salam et al., 2015).

32 Hypertensive disorders during pregnancy are a significant contributor to this perinatal morbidity and  
33 mortality (Khan et al., 2006). It has been reported that 10% of women have high blood pressure during  
34 pregnancy, and preeclampsia complicates 2% to 8% of all pregnancies (Duley, 2009). In low- and middle-  
35 income countries, results showed that overall, 10% to 15% of direct maternal deaths are associated with  
36 preeclampsia (Khan et al., 2006; Duley, 2009). Hypertensive disorders of pregnancy includes chronic  
37 hypertension, gestational hypertension, and preeclampsia, and there is substantial evidence that these  
38 lead to adverse outcomes both during pregnancy and after birth (Haas et al., 2019; Whelton et al., 2018;  
39 Mosca et al., 2011; Gooding et al., 2020; Powers et al., 2012; Boardman et al., 2020; Scheres et al., 2020;  
40 Berends et al., 2008; Wu et al., 2020; Parikh et al., 2017; Rich-Edwards et al., 2010; Melchiorre et al.,  
41 2011; Bergman et al., 2020; Catov et al., 2013). In particular, diverse outcomes related to hypertensive  
42 disorders of pregnancy can affect both mother and fetus in long- and short-term. They are associated with  
43 placental abruption, preterm delivery, fetal growth restriction, stillbirth, maternal death secondary to stroke  
44 and eclampsia, as well as future risk of hypertension, diabetes mellitus, and cardiovascular disease in the  
45 mother (ACOG, 2013). Moreover, blood pressure monitoring and management, has been shown to be  
46 beneficial during pregnancy (Scantlebury et al., 2013; Gillon et al., 2014; Magee et al., 2016; Podymow  
47 and August, 2017; Whybrow et al., 2020; Chawla et al., 2020). However, the majority of evidence is  
48 provided for populations in high-income settings. As Salam et al. (2015) noted, there is a need to improve  
49 low-cost screening of blood pressure and interventions for hypertensive disorders of pregnancy in low- and  
50 middle-income countries (LMICs), and to control preeclampsia in particular. This is expected to have a  
51 significant impact in preventing maternal and fetal mortality. The authors suggest the need to invest more  
52 in research at primary care level to improve the evidence base for community-level interventions.

53 Although numerous clinical and biochemical tests have been proposed for prediction or early detection  
54 of preeclampsia, most remain unrealistic for general use in LMICs (Wagner, 2004; Osungbade and Ige,  
55 2011). Challenges in the management of preeclampsia in low-resource settings include failure to identify  
56 preeclampsia along with a delay in responding to the clinical signs and symptoms due to the limited access  
57 to health care centers. For these reasons, routine blood pressure measurement in pregnancy is essential in  
58 the antenatal period. Therefore, designing low-cost and accessible monitoring systems, along with decision  
59 support, is essential to improving the quality of pregnancy care in LMICs, and improving patient outcomes.

60 While blood pressure monitoring is a key component to monitoring maternal-fetal well-being during  
61 pregnancy, it is important to note that it is also prone to errors, through incorrect usage, poor choice of  
62 device and arm cuff, poor body habitus and transcription or transmission errors (Mishra et al., 2013). In  
63 a related work, the authors demonstrated that even trained clinical experts make significant errors when  
64 transcribing basic medical information (Hall-Clifford et al., 2017). In the same work, they also showed that  
65 capture of data by mobile phones and tablets enabled them to reduce errors significantly, with only poor  
66 handwriting (that even the authors could not recognise at times, or remember writing), remaining as the  
67 barrier to accurate record keeping.

68 A number of wireless BP devices are now commercially available, with data transmission almost  
69 exclusively based on some variant of Bluetooth. Wireless handshaking is prone to connectivity errors due  
70 to radiofrequency interference, variations in standards, and non-causal activity on the phone (with various  
71 installed apps and services interfering with the connection). More importantly, to the best of the authors'  
72 knowledge, no BP devices with wireless connectivity have been validated in a preeclamptic population.  
73 The definitive work evaluating devices in such a population was performed by Bello et al. (2018), who  
74 identified only a very small number of devices which are appropriate for preeclampsia, and none with  
75 wireless connectivity. This presents a key problem for monitoring NP in pregnancy. Moreover, given the  
76 volume of legacy medical devices around the world which lack wireless connectivity, it is important that  
77 there is an efficient and reliable method for transcribing, reading, and transmitting data from standard BP  
78 devices. The virtually ubiquitous cellphone camera provides a potential scalable solution through optical  
79 character recognition (OCR). To-date there is no study evaluating the effectiveness of BP digitization, and  
80 its conformity with acceptable standards for use in clinical diagnosis, particularly for use in pregnancy.

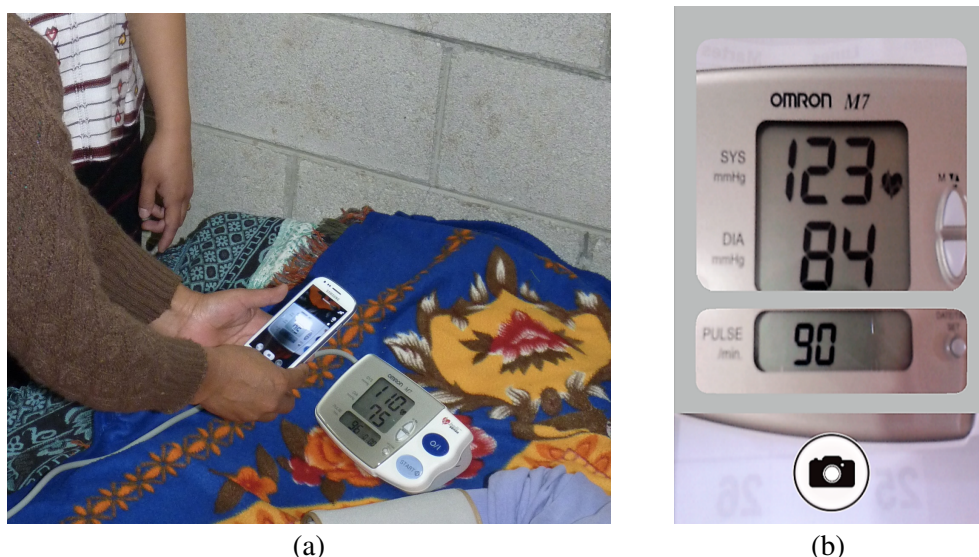


**Figure 1.** An Android-based app to capture blood pressure readings used in this study: Figure 1(a) shows the app being used by traditional birth attendants in Highland Guatemala (NBC Universal News Group, 2017). Figure 1(b) shows the app interface as seen by the user, with a 'mask' to help align the LCD and improve quality during capture.

81 In a recent step-wedge randomized control trial, the authors demonstrated that the introduction of blood  
82 pressure monitoring captured through an app led to improved outcomes in a mostly illiterate LMIC  
83 population Martinez et al. (2018). Through this work, the authors intend to automate the existing manual  
84 transcription of blood pressure. (It is important to note that the success of the proposed RCT was due  
85 to several factors to standardize blood pressure capture, which the authors address in more detail in the  
86 discussion.) In that RCT, an Omron M7 (Omron Co., Kyoto, Japan) automated oscillometric BP monitor  
87 was used by traditional birth attendants in Highland Guatemala to screen pregnant women for hypertension  
88 and preeclampsia in rural settings. The data presented here was drawn from the RCT, and so represents  
89 highly realistic field data. The Omron M7 was chosen because it has been validated in a preeclamptic  
90 population Bello et al. (2018). Figure 1(a) shows a traditional birth attendant capturing the data during  
91 a routine screening and a close-up of how the phone looks to the user during capture. BP readings were  
92 captured from the LCD screen using a standard cellphone camera and a bespoke Android app by traditional

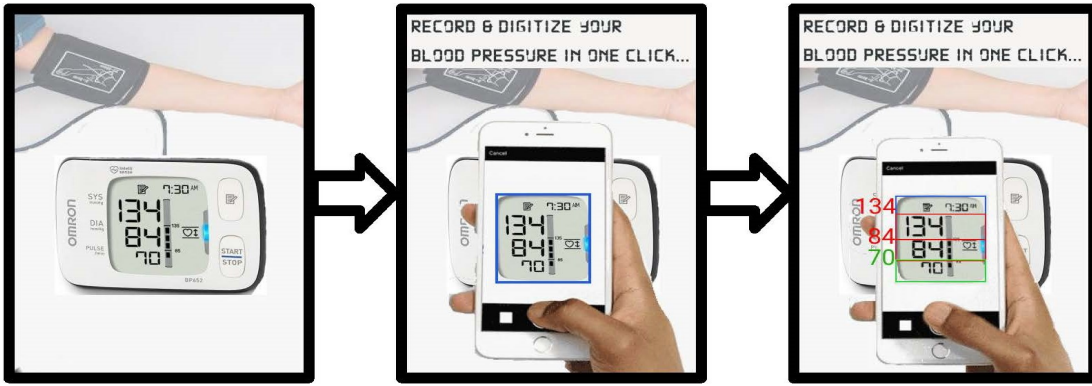


**Figure 2.** Steps of image transcription using cellphone camera

93 birth attendants during routine check-ups of patients (Figure 1(b)). Cellphone photographs of the display  
94 were used to train a deep learning approach to transcribe the readings into numerical values. An overview  
95 of the proposed approach can be seen in figure 2.

## 2 BACKGROUND ON NUMBER DIGITIZATION

96 Despite the increasing use of personal / electronic health records as well as smart and connected devices  
97 (e.g. via Bluetooth), the most widely employed method to record BP in clinical practice is through periodic  
98 manual transcription. Readings on automated BP devices are generally standardized with systolic and  
99 diastolic BP readings in large font and heart rate, date, time, and rhythm warnings in smaller letters (AHA,  
100 2020). This provides spatial context to assist image capture into a useful digital format via OCR. Although  
101 transcription is performed on both paper and smartphone applications, both methods are prone to reporting  
102 erroneous readings due to transcription and legibility errors, and patient recall bias (Hall-Clifford et al.,  
103 2017). Hence, a number of BP data logging methods (with and without wireless data transmission) have  
104 been investigated to enable automated BP management of patients. Some of these involve memory card-  
105 based storage (Omron Healthcare Inc, 2012) and USB transfer to a computer using commercial data logger  
106 software (Microsoft, 2007; Omron Healthcare Inc, 2014), mobile-based data logging app using Bluetooth  
107 (Omron Healthcare Inc, 2020) or Wi-Fi connectivity (Withings, 2020). However, wireless and cable  
108 connections introduce complications that reduce the number of readings that can be captured. In earlier  
109 work the authors showed that photos of medical data can help accurately capture such data (Hall-Clifford  
110 et al., 2017). This simple approach to logging BP readings using a smartphone app provides an easy,  
111 interactive and convenient method using familiar technology.

112 There have been a number of OCR algorithms developed over the years, stretching back to the 1980's and  
113 1990's, with a particular focus on machine learning approaches (Burr (1988); Matan et al. (1995); Lecun  
114 et al. (1995); Kim and Govindaraju (1997).) Work has also focused particularly on number recognition  
115 (Leelasantiham, 2009; Pham et al., 2018; Babbar et al., 2018). Approaches have also focused on building  
116 digital libraries through the process of extracting bibliographic data and inventorying details from book  
117 images (Kashimura et al., 1999; Chen et al., 2010), vehicular license plate recognition (Babbar et al., 2018),  
118 traffic sign recognition (Mammeri et al., 2014), and credit card number digitization (Leelasantiham, 2009).  
119 All these methods involve a pipeline of preprocessing, thresholding, delineation of area of interest using  
120 a template before finally applying character recognition in the localized region. Commercial OCR tools

121 have generally been optimized for scanner-captured documents rather than camera-captured documents  
 122 (Liang et al., 2004). For example, current PDF OCR tools include Google Drive OCR, Nuance, Adobe  
 123 Acrobat Reader and Readiris (Canon) (Pham et al., 2018). Image-based OCR tools include Tesseract  
 124 OCR(Tesseract (2005)), Abbyy Mobile OCR Engine and mobile applications such as CamScanner and My  
 125 Edison (Mammeri et al., 2014). Although some of these applications offer rapid and low-cost digitization  
 126 of data, their transcription accuracy decreases dramatically for images with geometrical distortions and  
 127 noise due to image acquisition and environmental factors (Liang et al., 2004). Moreover, the lack of open  
 128 research in these commercial systems makes assessment and repeatability of these approaches problematic.

129 Narrowing down the problem to only number digitization, there has been extensive research in handwritten  
 130 digit recognition (Ali et al., 2019) as well as credit card, and street-view imagery (Leelasantiham, 2009;  
 131 Goodfellow et al., 2013). Although a variety of classifiers have been used for this purpose, such as support  
 132 vector machine, k-nearest neighbors and neural networks, convolutional neural networks appear to provide  
 133 the best performance for digit recognition (Ali et al., 2019). In particular, Král and Čochner digitized analog  
 134 gas meter readings using meter localization, perspective correction and a digit-by-digit recognition using  
 135 Linear Support Vector classification and template matching methods (Král and Čochner, 2015). However,  
 136 very little research exists concerning the problem of LCD digit recognition. A relevant (non peer-reviewed)  
 137 computer vision project “Optimizer” developed by Izadi and Momeni (2018) used a deep learning approach  
 138 to digitize gas pump readouts. In that work, the authors proposed a digit-by-digit as well as a multi-digit  
 139 recognition approach (Goodfellow et al., 2013) to transcribe binarized segmented gas pump meter images  
 140 using a convolutional neural network (CNN). Another project digitized gaspump meters on a digit-by-digit  
 141 basis using a k-nearest neighbors approach (Kazmierczak, 2017) . However no statistics on how well these  
 142 approaches perform were provided. Moreover, when these works were evaluated on the data in the study,  
 143 they produced poor results.

144 Never-the-less, there is clear potential in modern CNN-based approaches, and in this work the authors  
 145 propose an image-based OCR approach using CNN which shares some similarities to the works presented  
 146 by Goodfellow et al. (2013) and Izadi and Momeni (2018).

### 3 METHODS

147 In this section the step-by-step approach to convert BP monitor images into computer-readable numerical  
 148 format is described, including localization, extraction and recognition of the images. The end-to-end  
 149 workflow can be found in Figure 3.

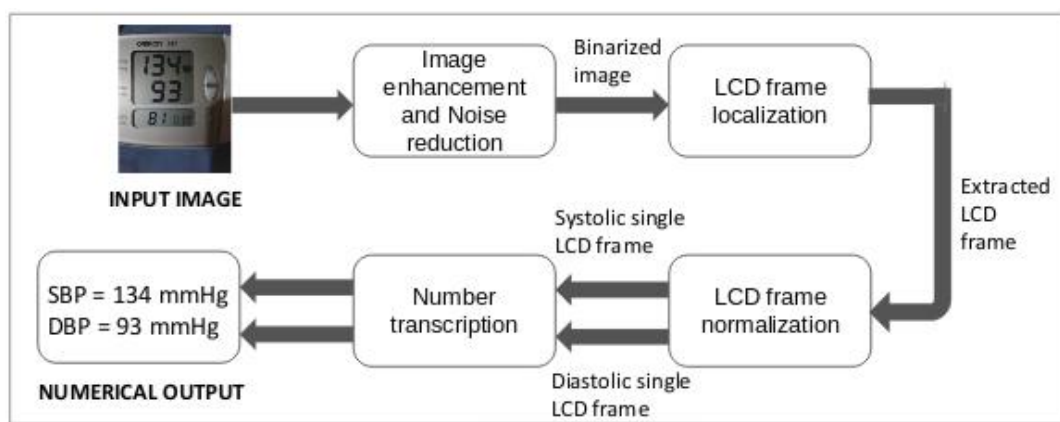


**Figure 3.** Design of Proposed OCR approach to digitize blood pressure readings.

### 150 3.1 Database

151 Data used in this work were collected as a part of a randomized control trial in collaboration with  
152 lay midwives on improving access to obstetrical care conducted in rural highland Guatemala in the  
153 vicinity of Tecpan, Chimaltenango. This trial was approved by the Institutional Review Boards of Emory  
154 University, the Wuqu Kawoq | Maya Health Alliance, and Agnes Scott College (Ref: Emory IRB00076231  
155 - ‘Mobile Health Intervention to Improve Perinatal Continuum of Care in Guatemala’) and registered on  
156 ClinicalTrials.gov (identifier NCT02348840). More details on the design and implementation of the data  
157 collection system, and the training of the traditional birth attendants can be found in Stroux et al. (2016),  
158 Martinez et al. (2018) and Martinez et al. (2017).

159 At each visit, a traditional birth attendant recorded at least two maternal BP readings using the Omron M7  
160 self-inflating device (Omron Healthcare Europe BV, Hoofddorp, the Netherlands). With specific reference  
161 to the conditions for capturing images, all visits were conducted inside the mother’s home, where lighting  
162 was generally poor, but highly variable. No prescription was given for adjusting lighting conditions or use  
163 of flash. The user was trained to align the image using a ‘mask’ that appears to resemble the monitor (see  
164 figure 5), and retake if they were not happy with the result in terms of readability due to focus, lighting,  
165 cropping or scale. The request to iterate until the users considered the images useful created an inflated  
166 representation of low quality images in the given database compared to the number of visits, but also led  
167 to readable data for most visits. Each BP estimate was assessed on both of the subject’s arms while the  
168 patient was in the supine position. (The position was chosen to minimize changes in traditional practices as  
169 it produces a small offset in mean blood pressure, and reduces variability due to body habitus (Martinez  
170 et al., 2017).) Once a BP reading was taken, the midwife registered the BP on a mobile app by taking a  
171 picture of the device screen. The mobile phone models used in this study were Samsung Galaxy S3 or  
172 J2. The matrix size/resolution of the images was 640x480 pixels. The spatial resolution depended on the  
173 distance of the camera from the blood pressure device. The size of the detected blood pressure LCD ranged  
174 from 137x146 to 264x303 pixels. The physical size of the Omron M7’s number display is 2.5 x 2.5cm (for  
175 the blood pressure) and 2.5cm x 1.3cm for the heart rate section. The numbers are 1.9 cm high by 1.25 cm  
176 wide for blood pressure and 0.64 cm high by 0.42 cm wide for heart rate.

177 Between January 2013 and July 2019, a total of 8,192 images were captured from 1,697 pregnant women  
178 carrying singletons between 6 weeks and 40 weeks gestational age. The systolic blood pressure (SBP),  
179 diastolic blood pressure (DBP), and heart rate (HR) of each BP image were manually transcribed by two  
180 independent annotators, storing the data in independent locations inaccessible to the other. Annotators  
181 screened each of the images for readability, as well as image quality labels. Readability was defined as the  
182 ability to clearly transcribe the full numerical values of the SBP, DBP and HR. If a value for any of these  
183 parameters could not be transcribed, one of the following labels was assigned to the image, which was then  
184 replaced as a ‘not a number’ (NaN) during preprocessing.

- 185 • **Out of Focus, Fully Captured.** The image was out of focus/ blur, and it was not possible to identify  
186 SBP, DBP, as well as the HR values by a human. The image was annotated as ‘O’.
- 187 • **Contains Something Other than Blood Pressure.** The image contained something other than BP  
188 monitor but was not personally identifiable. The image was annotated as ‘N’.
- 189 • **Too Dark.** The image was too dark, and it was not possible to read SBP, DBP and/or HR values by a  
190 human. The image was annotated as ‘D’.
- 191 • **Contains Reflections.** The image contained strong reflections due to illumination challenging the  
192 identification of its values. The image was annotated as ‘R’.

- 193 • **File is Corrupt.** The image file cannot be opened and was annotated as label ‘C’.  
194 • **Contains Something Personally Identifiable Other than the Blood Pressure Data.** The image  
195 contained something other than the BP device screen that was personally identifiable - ear, eye, tattoo,  
196 identity card, fingerprint, etc. The image was annotated as ‘P’.
- 197 Sampling an average of four images per mother, distributed evenly over the 41 midwives who captured  
198 the data, a total of 7205 images were annotated for the values of SBP, DBP, HR along with a quality label.  
199 The defined quality labels are as follows:
- 200 • **Blurred.** The image was out-of-focus/blur making it difficult to interpret values of SBP, DBP and HR.  
201 The quality label given was ‘B’.  
202 • **Dark.** The image lighting conditions were dark even if the values could be manually transcribed. The  
203 quality label given was ‘D’.  
204 • **Contains Reflections.** The image contained reflections due to illumination variation, reflection from  
205 LCD screen or from cellphone camera even if image is readable. The quality label given was ‘R’.  
206 • **Far.** The BP monitor was excessively distant from the camera or zoomed out, leading to only a small  
207 region of the image / number of pixels representing the blood pressure reading. The quality label given  
208 was ‘FAR’.  
209 • **Cropped** The image LCD screen (region of interest) was cropped, but the all the values were visible.  
210 The quality label given was ‘CROPPED’.  
211 • **Good Quality.** The image had readable numbers without any quality issues described above. The  
212 quality label given was ‘OK’.

213 Examples of images with each quality label can be seen in Figure 4.

214 As the annotation process was manual, it may have been affected by typos and other human errors. To  
215 remove annotation errors, once the two annotators transcribed all the BP images, a third independent  
216 annotator reviewed those BP images in which the two annotators disagreed. Thus, the third annotator  
217 corrected any annotation error and generated the final spreadsheet used in this work. Segregation of these  
218 7205 images based on their quality metric yielded 740 “Blur” quality images, 314 “Dark” quality images,  
219 3885 images containing reflections, 375 “Far” images, 630 “Cropped” images and 1261 “Good Quality”  
220 images. Further, for the purpose of the analysis presented in this study, the authors categorized all these  
221 images into two categories: Good Quality images(Inclusive of images with “OK” quality label) and poor  
222 quality images(Inclusive of images with “Blur”, “Dark”, “Far”, “Contains Reflections” “Cropped” quality  
223 labels)

### 224 3.2 Preprocessing

225 Given the wide variability in the appearance of the BP monitor images due to orientation, zooming,  
226 environmental factors like lighting, shadows, noise, as well as image acquisition factors like motion,  
227 out-of-focus and in-focus blurs as given in the previous section, preprocessing of the images was required  
228 before extracting the region of interest. The authors used OpenCV library (Bradski, 2000) for this purpose.

229 It can be noted that the digits on the BP LCD are not continuous (i.e. they are made of seven segments)  
230 and therefore have some similarities to halftone documents. Halftone documents are printed with one  
231 color of ink, in dots of differing size (pulse-width modulation) or spacing (frequency modulation), or  
232 both. This creates an optical illusion and when the half-tone dots are small, the human eye interprets the

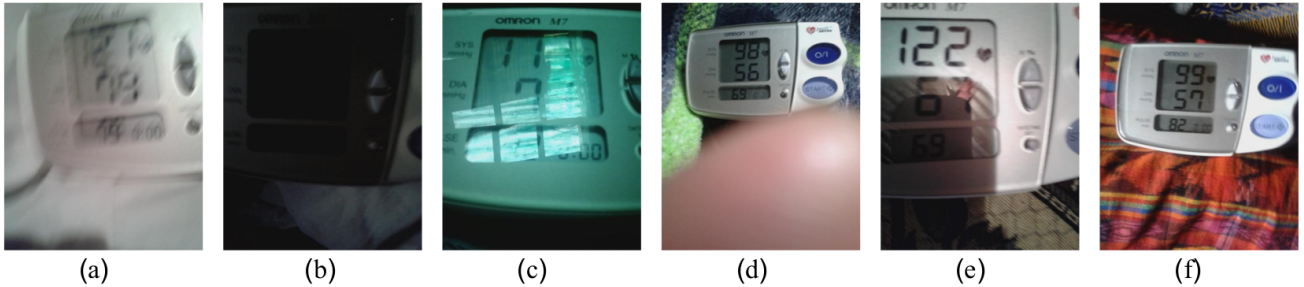


**Figure 4.** Examples of each class from blood pressure images dataset. a) Blur. b) Dark. c) Contains reflections. d) Far. e) Cropped. f) Good quality.

233 patterned areas as if they were smooth tones. As Adak et al. (2015) pointed out, classical binarization  
 234 techniques on half-tone images do not produce the standard output for feeding into the OCR engine and  
 235 need further processing. However, because the BP LCD more closely resembles text with artifacts of  
 236 missing connectivity in a digit or letter than half-tone documents, which have a more uniform missing  
 237 pattern, the authors expect that a different preprocessing approach is needed.

### 238 3.2.1 Image enhancement

239 The first module of the proposed preprocessing algorithm involved enhancing the LCD frame boundaries  
 240 in the image and thresholding it to enable accurate extraction of the BP and heart rate LCD frames from the  
 241 images shown in the next module. For this, the image was first converted to grayscale. This step allowed  
 242 faster processing of the images, saving on computation resources due to reduced size and number of  
 243 channels. Next, it was fed to a bilateral filter to smooth the images while preserving edges (Bradski, 2000)  
 244 followed by gamma correction to correct illumination levels in the image using non linear transformation  
 245 between the input pixel values and the mapped output pixel values given by(Bradski, 2000):

$$O = \left( \frac{I}{255} \right)^{\gamma} * 255 \quad (1)$$

246 Binarization is the process of conversion of image using a threshold such that all of its pixels either take  
 247 value 0 or 1.This step is essential in LCD frame extraction to obtain clearly defined frame boundaries as well  
 248 as clearly defined digits contributing to overall accuracy of the OCR. Given the variance in image quality,  
 249 the above adjustment regime was not enough for thresholding all images into their binary counterparts  
 250 using a global threshold value. Hence, the authors decided to adopt the adaptive thresholding technique,  
 251 wherein a threshold is calculated over small pixel neighborhood regions of image. Since different thresholds  
 252 exist for different regions of the same image, this approach gave better accuracy for images with varying  
 253 lighting and environmental conditions (Bradski, 2000).

### 254 3.2.2 LCD frame localization

255 In this module, the BP and heart rate LCD frames were localized in the preprocessed image. Initially,  
 256 the authors started inspecting simple contour attributes like width, height, center, size and area. Due to  
 257 orientation and zooming effects of the images, the size and the location of the LCD frames differed over  
 258 a wide range in the preprocessed images. For example, the images annotated with quality label “FAR”  
 259 had a small random portion of the image occupied by the BP monitor, while the images with quality label  
 260 “CROPPED” had a cropped section of the BP monitor. In addition to that, the high amount of noise at  
 261 the frame location due to environmental and image acquisition factors made the contour area unsuitable

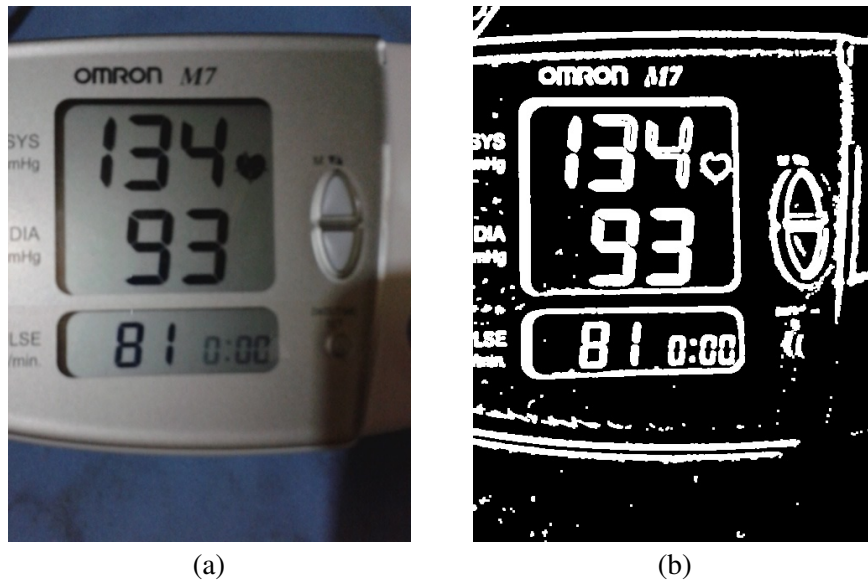


**Figure 5.** Figure 5(a) shows a sample input RGB image while Figure 5(b) shows the binary thresholded image obtained after performing Image enhancement on the input.(See Section 3.2.1)

262 for LCD frame localization. Hence, in order to support the size attribute of the contours to localize LCD  
 263 frames, the authors decided to inspect the aspect ratio of all the contours detected in the image. The  
 264 aspect ratio of an object is the ratio of width/height of the object. Based on experiential analysis of these  
 265 attributes for nearly 500 images chosen at random, the thresholds to localize the LCD frames were decided.  
 266 Due to relatively smaller size of the heart rate LCD frame, the authors then corrected its 4 bounding box  
 267 coordinates by verifying the corresponding 4 coordinates of BP LCD frame bounding box.

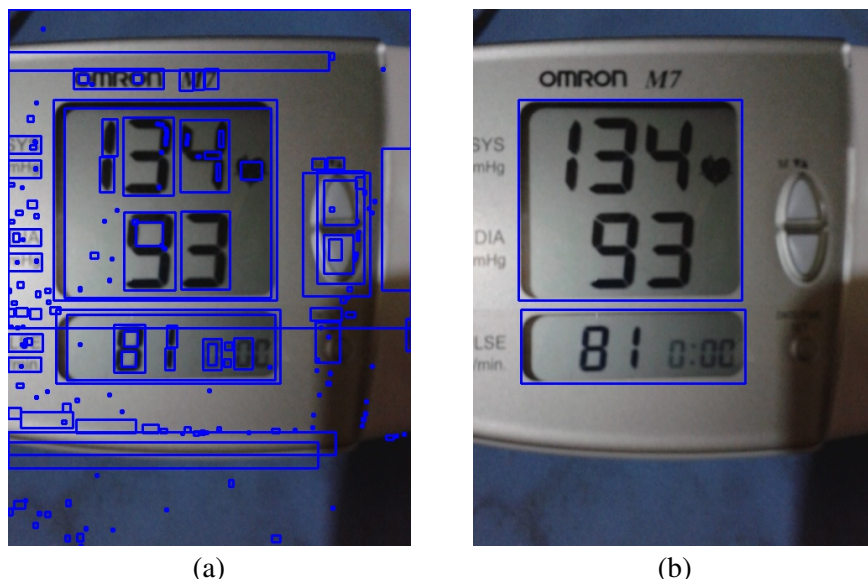


**Figure 6.** Figure 6(a) displays all possible contours on enhanced image and figure 6(b) shows the localized region of interest obtained using LCD localization (See Section 3.2.2)

268 3.2.3 LCD frame normalization

269 The obtained BP and heart rate LCD frames differed in sizes because of the differences in distance of the  
 270 camera from the BP monitor. Hence, the authors normalized each of the frames to a fixed size using scaling.  
 271 The bounding boxes extracted from the images included the boundary of the LCD. A simple approach to  
 272 discard these boundaries by removing certain rows and columns along the boundary of the normalized  
 273 LCD images was adopted. The row and column removal thresholds were decided through analysis on  
 274 nearly 500 random images from the dataset, as validated by the work presented by Shah et al. (2009). Each  
 275 of the BP LCD frames were further divided into half along vertical height, to get systolic BP and diastolic  
 276 BP LCD images. This sequence of single LCD binary images were fed to the number transcription model.

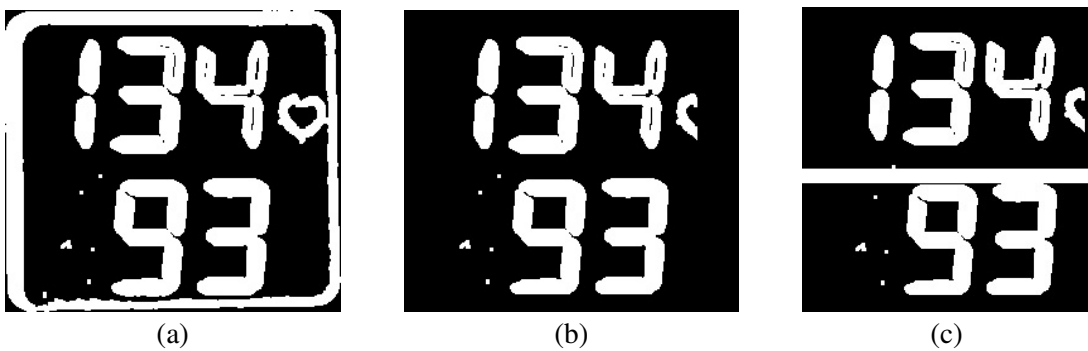


**Figure 7.** Figure 7(a) shows the binary thresholded BP LCD frame extracted with contour border while Figure 7(b) shows the LCD frame after border removal. Figure 7(c) shows 2 single monitor LCD frames as a final result of the LCD Normalization module.(See Section 3.2.3)

277 3.3 Number transcription using Convolutional Neural Networks

278 Transcription of medical device display values is a sequence recognition problem. Given the image of a  
 279 medical device display, the task is to identify the BP readings in the LCD frame extracted from the image.  
 280 These values are a sequence of digits where the accuracy of transcription depends on estimating the entire  
 281 value and not individual digits independently. This is because a variation in a single digit has a significant  
 282 effect on the estimated BP value proportional to the order of the magnitude of the digit. Hence, the authors  
 283 based their system on the unified multi-digit recognition approach proposed by Goodfellow (Goodfellow  
 284 et al., 2013).

285 In the study, the authors proposed a CNN based approach that simultaneously learned (*i*) the digits and  
 286 (*ii*) where to look for them. The digits were then recognized based on the coverage at certain levels of  
 287 accuracy obtained using a confidence threshold. The confidence threshold is the probability of the most  
 288 likely prediction being correct. Thus, by representing the blood pressure value as a sequence of digits  
 289 ( $s = s_1, s_2, \dots, s_n$ ), the aim was to train a probabilistic model of sequences given images. Hence, for output  
 290 sequence  $S$  of  $N$  random variables (one per digit) given input image  $X$ , a probabilistic model  $P(S|X)$   
 291 would be learned by maximizing the log  $P(S|X)$  on the training data. Given that the maximum value  
 292 of BP is a 3-digit number, the length of the sequence  $s$  was chosen to be 3. Also, since each of the digit  
 293 variables could take a finite number of possible values (0 to 9), a softmax classifier could be used to get  
 294 each of the digits, where input of classifier are the features extracted from  $X$  using the CNN. Using the  
 295 back-propagation learning rule the digit classifier would then generate the digits and not return anything  
 296 if no digit is predicted. In this proposed study, a 180 x 80 input vector was fed to three-layer CNN with  
 297 32, 64 and 128 filters of dimension 5x5 to extract features from the corresponding feature vector. Each

layer was followed by a batch normalization, ReLU activation and maxpooling layer. The output feature vector from the CNN was then fed to a softmax classifier with three output channels, corresponding to the estimate for each of the three possible digits (Izadi and Momeni, 2018).

### 3.4 Experiments

The entire dataset was first balanced to create an equal number of systolic and diastolic single LCD frames. The high variance in the number of images of different quality meant that dataset balancing with respect to quality was not considered in current study. Both good quality and bad quality images were divided into training and test data in the ratio 3:1 to train and evaluate the performance of models developed in each experiment. A total of 542 good quality images and 1693 poor quality images comprised the test dataset, which were not used during any training or optimization.

#### 3.4.1 Experiment 1

In order to produce a baseline result to compare to the proposed approach, the authors used ‘Tesseract’, one of the most accurate open-source OCR engines. Originally developed at Hewlett-Packard in the mid 1980s, it has been maintained by Google since 2006 (Smith, 2007; Tesseract, 2005). Tesseract OCR is free and released under the Apache V2.0 open source license. No training was performed to optimize the parameters of the algorithm. However, the software was applied at each stage of preprocessing pipeline proposed in this work (as well as on raw data), and the best results were reported.

#### 3.4.2 Experiment 2

The authors also compared their proposed method with the commercial state-of-the-art model provided by Google for OCR to transcribe text from images known as Google Vision API (Google, 2020). While no public performance statistics are available for the Google Vision model, it is widely used by developers and therefore is perhaps the best ‘public’ comparison with the proposed approach. It should be noted that Google vision API is not free for commercial use and it offers a limited number of API calls, after which payment must be made. This can be cost-prohibitive for many applications in low-resource contexts. Moreover, the algorithm requires processing in the cloud, which is not feasible in low resource regions of the world due to poor internet connectivity issues, and may be illegal or unethical in a medical context. Again, the Google Vision API was applied to both raw and the preprocessed test images generated through the study, and the best performance was reported. No retraining of Google’s API was possible.

#### 3.4.3 Experiment 3

In this experiment, the proposed model was trained only on the good quality images by further dividing remaining good quality images into training and validation data in the ratio 3:1 and the best model was obtained by setting a model checkpoint on the incurred validation loss. The trained model was then tested on the held-out good quality images as well as the held-out poor quality images to validate its performance on images of different quality.

#### 3.4.4 Experiment 4

In this experiment, the proposed model was trained on both the good quality and poor quality images by combining the remaining good quality and bad quality images together. The dataset formed was then divided into training and validation data in the ratio 3:1, keeping equal percentage of contributions from good and poor quality images. The best model was obtained by setting a model checkpoint on the incurred validation loss. The trained model was then tested on the held-out good quality images as well as the

338 held-out poor quality images to evaluate its performance on images of different quality and compare its  
339 performance to the other approaches described in this work.

## 4 RESULTS

### 340 4.1 Preprocessing

341 Given an input BP monitor image, the preprocessing module returned systolic and diastolic BP single  
342 monitor binary thresholded LCD frames. The process of obtaining the output through the serialized  
343 execution of 3 steps described in the previous section can be observed in Figures 5, ?? and 7. An LCD  
344 frame extraction accuracy of 85% was observed after the preprocessing module on the good quality images.  
345 On the other hand only 57.8% of poor quality images were extracted into their systolic and diastolic LCD  
346 counterparts.

### 347 4.2 Performance of each classification approach

348 In experiment 1 and 2, Tesseract OCR engine and Google vision API were used to transcribe the held  
349 out test dataset respectively. In experiment 3, the proposed model was trained on 1082 good quality single  
350 LCD images and was validated on 540 good quality images to obtain the best possible CNN for the dataset.  
351 While in experiment 4, the model was trained on 5020 images (all single LCD images except those in  
352 unknown test dataset) and its best possible solution was obtained through validation on 1677 images (all  
353 single LCD images except those in unknown test dataset).

354 Table 1 shows the results for classifying the images for the specified experiments. The results of the  
355 experiment 1 demonstrates that Tesseract OCR engine accuracy is around 17% for good quality and and  
356 7% for poor quality images. Experiment 2 shows that Google’s Vision API can only achieve an accuracy of  
357 approximately 42% and 24% for good and poor quality images respectively, with mean absolute errors of  
358 between 36 mmHg and almost 89 mmHg, which is far outside any acceptable bounds. This shows that  
359 Tesseract and Google’s OCR system are unable to produce usable results and introduces significant errors  
360 into the digitization in this scenario. Experiments 2 and 3 achieved similar accuracy rates for classifying  
361 good and poor quality images, although training with both good and poor quality images generally provided  
362 a marginal boost in performance on both types of images. Specifically, systolic and diastolic good quality  
363 images obtained a higher accuracy around 90% for both experiments, whereas the poor quality images  
364 yielded an accuracy around 63%.

## 5 DISCUSSION AND CONCLUSIONS

365 The method proposed in this work is a novel implementation for digitizing LCD numbers. Although the  
366 use of a CNN has previously been proposed for digitizing similar digits from gas meters, it remained  
367 unpublished, apart from as a GitHub repository. The works lacked any assessment of performance, or  
368 peer-review. Moreover, the authors were unable to produce any useful results from the methods presented,  
369 despite the availability of the code. As such, that work cannot be considered a predicate, and unfortunately,  
370 in the authors’ experience, is representative of the state of much of the code and websites posted today.  
371 In contrast, this work provides a strong empirical analysis of their pipeline, which includes a significant  
372 amount of preprocessing to improve the quality of the images. The final method provides a low error for  
373 digitizing blood pressure which is well within the FDA guidelines of 5 mmHg, (Ruzicka et al., 2016),  
374 making it suitable for general use. The performance of the proposed method were also investigated using

**Table 1.** OCR performance. For each experiment, the classification accuracy and the mean absolute error (MAE) is provided for the image sets. DBP indicates diastolic blood pressure and SBP indicates systolic blood pressure. Best performance statistics are in bold.

Experiment	Training	Test data	Classification accuracy (%)	MAE (mmHg)
1	Tesseract	Held-out good quality images (SBP)	20.2	185.2
		Held-out good quality images (DBP)	14.3	49.3
		Held-out poor quality images (SBP)	6.7	191.8
		Held-out poor quality images (DBP)	7.9	52.8
2	Google Vision API	Held-out good quality images (SBP)	42.1	64.03
		Held-out good quality images (DBP)	43.2	36.46
		Held-out poor quality images (SBP)	26.5	88.57
		Held-out poor quality images (DBP)	23.0	56.47
3	CNN model, Good quality images	Held-out good quality images (SBP)	88.1	<b>2.29</b>
		Held-out good quality images (DBP)	86.1	1.73
		Held-out poor quality images (SBP)	61.7	7.55
		Held-out poor quality images (DBP)	62.8	5.03
4	CNN model, Good and Poor quality images	Held-out good quality images (SBP)	<b>90.7</b>	3.19
		Held-out good quality images (DBP)	<b>91.1</b>	<b>0.94</b>
		Held-out poor quality images (SBP)	65.1	8.00
		Held-out poor quality images (DBP)	66.2	3.69

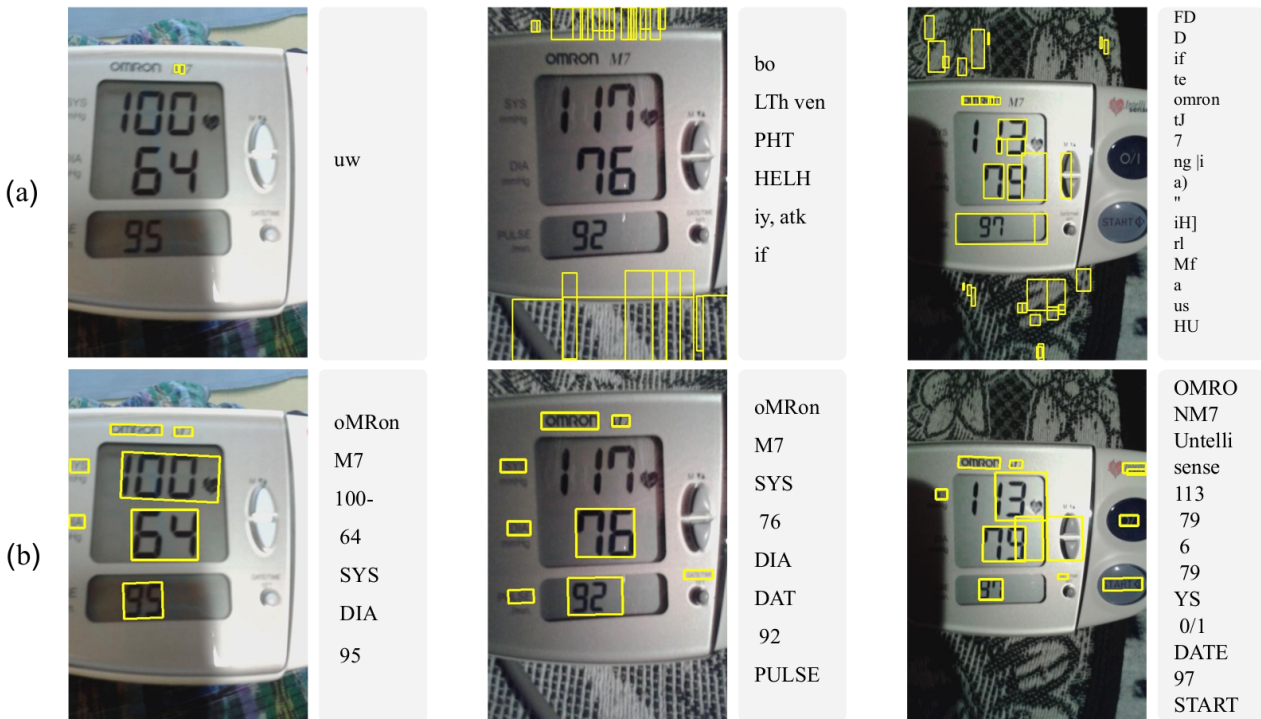


**Figure 8.** Three typical examples of OCR results using 8(a) Tesseract and 8(b) Google vision API on original (raw) good quality images. Notice the significant errors produced by Tesseract with overwhelming false positive and negative detections, resulting in no useful information. The Google API produced acceptable results on only one of the photographs.

375 different CNN structures. However less complex networks degraded the results. More complex networks  
376 and more data may, therefore, improve results.

377 Commercial state-of-the art approaches produced unacceptable results with extremely large errors on  
378 the blood pressure images in this study. Figure 8 provides typical results, with transcription errors such  
379 as identification of non-digits as text (false positives), missing digits (false negatives), and inconsistent  
380 formatting of the text, making post-processing extremely difficult, or impossible.

381 The authors note several limitations of their work. Performance on low quality data was poor, as expected  
382 - if the numbers in an image are cut off, or it contains substantial reflections that obscure the number, then  
383 there is little hope of an accurate transcription. The only way to correct such errors is at the point of capture.  
384 It is therefore important to develop an algorithm to identify the quality of an image that can run on the  
385 cellphone. Future work will be aimed at the development of such an approach using the extensive labelled  
386 database used in the study that can pre-select between unreadable and readable data, so that the system can  
387 feedback this information to the user. However, it is interesting to note that modern cameras such as the  
388 Google Pixel and the Samsung S10 series already have such software built-in. Therefore, in the coming  
389 years, as this technology trickles down to lower cost phones, there may be no need to develop additional  
390 methods, and the technology presented here is likely to be integrated into future phones as standard.

391 A classic seven-segment digital display is standardized for many LCD interfaces on medical devices and  
392 different sizes of digits should not affect the analysis, since the CNN allows for scaling. However, there is a  
393 lower resolution limit where the phone may be too far from the device and the resolution would be too low.  
394 Also, BP numbers displayed in a color format would not affect the digitization process as it thresholds and  
395 converts the image into a binary image before feeding it to the model. However, for using blood pressure  
396 devices with different fonts the network should be retrained.

397 As noted in the introduction, there are other issues that can affect BP accuracy in the field, including  
398 incorrect usage, poor choice of device and arm cuff, poor body habitus and transcription or transmission  
399 errors (particularly in low literacy populations). While the presented work only addresses the latter, the  
400 authors have demonstrated that the other issues can be mitigated with only a limited amount of training in  
401 a low literacy population Martinez et al. (2018).

402 In particular, through a co-design process Stroux et al. (2016); Martinez et al. (2017), the authors adapted  
403 the interface of the phone, and the training procedures to the local population's practices, such as patient  
404 review while supine. It is important to note that the success of the RCT was due to several factors in  
405 addition to standardized blood pressure capture, as a result of this preparatory fieldwork. This included  
406 building a multichannel communication modality (SMS, voice, GPRS and WiFi) linked to a coordinator  
407 who was able to deploy 'care navigators' (Martinez et al., 2018). Never-the-less, the step-wedge nature of  
408 the assessment indicates that without the technology, manual transmission of information provided poorer  
409 outcomes.

410 The proposed method is also highly generalizable and applies to a wide range of devices, beyond the  
411 blood pressure cuffs such as monitoring glucose level in diabetics populations. (Low cost blood glucose  
412 devices typically have LCD displays and no connectivity which makes them well suited for the application  
413 of the proposed method.) The algorithmic complexity of the system put forth by the authors is low enough  
414 to allow deployment on most modern Android smartphones using the TensorFlow Lite Android Support  
415 Library. The proposed method can therefore provide a first-line decision support mechanism for individuals  
416 or healthcare workers with little training. The connected nature of the phone can allow subsequent review  
417 to flag errors and provide a continually evolving and improving system.

418 In conclusion, the authors have presented evidence to show that the use of an app employing the methods  
419 described in this article may improve outcomes. However, an RCT is required to determine the veracity  
420 of this hypothesis. Since, they have developed the framework for such an RCT with the community with  
421 which they developed the system, they hope to implement the system on a phone using tensorflow lite and  
422 assess its impact in future work.

## ACKNOWLEDGMENTS

423 This work was supported by the National Science Foundation, Award 1636933 (BD Spokes: SPOKE:  
424 SOUTH: Large-Scale Medical Informatics for Patient Care Coordination and Engagement) and the National  
425 Institutes of Health, the Fogarty International Center and the Eunice Kennedy Shriver National Institute of  
426 Child Health and Human Development, grant number 1R21HD084114-01 (Mobile Health Intervention  
427 to Improve Perinatal Continuum of Care in Guatemala). GC is also supported by the National Center for  
428 Advancing Translational Sciences of the National Institutes of Health under Award Number UL1TR002378.  
429 The content is solely the responsibility of the authors and does not necessarily represent the official views of  
430 the National Institutes of Health or National Science Foundation. This work was part of a study approved by  
431 the Institutional Review Boards of Emory University, the Wuqu' Kawoq | Maya Health Alliance, and Agnes  
432 Scott College (Ref: Emory IRB00076231 - 'Mobile Health Intervention to Improve Perinatal Continuum  
433 of Care in Guatemala') and registered as a clinical trial (ClinicalTrials.gov identifier NCT02348840).

## REFERENCES

- 434 ACOG (2013). Hypertension in pregnancy: Report of the American College of Obstetricians and  
435 Gynecologists' task force on hypertension in pregnancy.
- 436 Adak, C., Maitra, P., Chaudhuri, B. B., and Blumenstein, M. (2015). Binarization of old halftone text  
437 documents. In *TENCON 2015 - 2015 IEEE Region 10 Conference*. 1–5
- 438 AHA (2020). My Blood Pressure Log - American Heart Association. <https://www.heart.org/-/media/files/health-topics/high-blood-pressure/my-blood-pressure-log.pdf>. Accessed: March 15, 2020
- 441 Ali, S., Shaukat, Z., Azeem, M., Sakhawat, Z., Mahmood, T., and Rehman, K. (2019). An efficient and  
442 improved scheme for handwritten digit recognition based on convolutional neural network. *SN Applied  
443 Sciences* 1
- 444 Babbar, S., Kesarwani, S., Dewan, N., Shangle, K., and Patel, S. (2018). A new approach for vehicle  
445 number plate detection. In *2018 Eleventh International Conference on Contemporary Computing (IC3)*  
446 (IEEE), 1–6
- 447 Bello, N. A., Woolley, J. J., Cleary, K. L., Falzon, L., Alpert, B. S., Oparil, S., et al. (2018). Accuracy  
448 of blood pressure measurement devices in pregnancy: a systematic review of validation studies.  
449 *Hypertension* 71, 326–335
- 450 Berends, A. L., De Groot, C. J., Sijbrands, E. J., Sie, M. P., Benneheij, S. H., Pal, R., et al. (2008). Shared  
451 constitutional risks for maternal vascular-related pregnancy complications and future cardiovascular  
452 disease. *Hypertension* 51, 1034–1041
- 453 Bergman, L., Nordlöf-Callbo, P., Wikström, A. K., Snowden, J. M., Hesselman, S., Edstedt Bonamy,  
454 A. K., et al. (2020). Multi-Fetal Pregnancy, Preeclampsia, and Long-Term Cardiovascular Disease.  
455 *Hypertension* 76, 167–175
- 456 Boardman, H., Lamata, P., Lazdam, M., Verburg, A., Siepmann, T., Upton, R., et al. (2020). Variations in  
457 Cardiovascular Structure, Function, and Geometry in Midlife Associated with a History of Hypertensive  
458 Pregnancy. *Hypertension* 75, 1542–1550
- 459 Bradski, G. (2000). The OpenCV Library. *Dr. Dobb's Journal of Software Tools*
- 460 Burr, D. J. (1988). Experiments on neural net recognition of spoken and written text. *IEEE Transactions  
461 on Acoustics, Speech, and Signal Processing* 36, 1162–1168
- 462 Catov, J. M., Lewis, C. E., Lee, M., Wellons, M. F., and Gunderson, E. P. (2013). Preterm birth and future  
463 maternal blood pressure, inflammation, and intimal-medial thickness: The CARDIA study. *Hypertension*  
464 61, 641–646

- 465 Chawla, R., Madhu, S. V., Makkar, B., Ghosh, S., Saboo, B., and Kalra, S. (2020). RSSDI-ESI clinical  
466 practice recommendations for the management of type 2 diabetes mellitus 2020. *Indian Journal of  
467 Endocrinology and Metabolism* 24, 1
- 468 Chen, D., Tsai, S., Girod, B., Hsu, C.-H., Kim, K.-H., and Singh, J. (2010). Building book inventories  
469 using smartphones. In *Proceedings of the 18th ACM international conference on Multimedia*. 651–654
- 470 Duley, L. (2009). The global impact of pre-eclampsia and eclampsia. In *Seminars in Perinatology*  
471 (Elsevier), vol. 33, 130–137
- 472 Gillon, T. E., Pels, A., Von Dadelszen, P., MacDonell, K., and Magee, L. A. (2014). Hypertensive disorders  
473 of pregnancy: A systematic review of international clinical practice guidelines. *PLoS ONE* 9
- 474 Goodfellow, I., Bulatov, Y., Ibarz, J., Arnoud, S., and Shet, V. (2013). Multi-digit Number Recognition  
475 from Street View Imagery using Deep Convolutional Neural Networks
- 476 Gooding, H. C., Gidding, S. S., Moran, A. E., Redmond, N., Allen, N. B., Bacha, F., et al. (2020).  
477 Challenges and Opportunities for the Prevention and Treatment of Cardiovascular Disease Among  
478 Young Adults: Report From a National Heart, Lung, and Blood Institute Working Group. *Journal of the  
479 American Heart Association* 9
- 480 Google (2020). Google vision API. <https://cloud.google.com/vision/docs/ocr>
- 481 Haas, D. M., Parker, C. B., Marsh, D. J., Grobman, W. A., Ehrenthal, D. B., Greenland, P., et al. (2019).  
482 Association of Adverse Pregnancy Outcomes With Hypertension 2 to 7 Years Postpartum. *Journal of  
483 the American Heart Association* 8
- 484 Hall-Clifford, R., Roche, S., Fathima, S., Palmius, N., Hollingworth, K., Kennedy, J., et al. (2017).  
485 Sustainable Technology for Surgical Referrals: Pilot Implementation of an Electronic Referral System  
486 for Short-Term Surgical Missions. *Journal of Health Informatics in Developing Countries* 11
- 487 Izadi, S. and Momeni, A. (2018). Seven-Segment-OCR. <https://github.com/SachaIZADI/Seven-Segment-OCR>
- 488 Kashimura, M., Ozawa, S., Onda, N., and Yang, H. (1999). Extraction of Bibliography Information Based  
489 on Image of Book Cover. In *Image Analysis and Processing, International Conference on* (Los Alamitos,  
490 CA, USA: IEEE Computer Society), 921
- 491 Kazmierczak, K. (2017). GasPumpOCR. <https://github.com/kazmiekr/GasPumpOCR>
- 492 Khan, K. S., Wojdyla, D., Say, L., Gülmезoglu, A. M., and Van Look, P. F. (2006). WHO analysis of  
493 causes of maternal death: a systematic review. *The lancet* 367, 1066–1074
- 494 Kim, G. and Govindaraju, V. (1997). A lexicon driven approach to handwritten word recognition for  
495 real-time applications. *IEEE Transactions on Pattern Analysis and Machine Intelligence* 19, 366–379
- 496 Král, P. and Čochner, M. (2015). Gas measurement in Paralelni Polis. <https://github.com/ParalelniPolis/pplyn>
- 497 Lecun, Y., Jackel, L., Bottou, L., Brunot, A., Cortes, C., Denker, J., et al. (1995). Comparison of learning  
498 algorithms for handwritten digit recognition. In *International Conference on Artificial Neural Networks*
- 499 Leelasanthiam, A. (2009). A System for Checking Code Numbers on a Credit Card and a Paper of Personal  
500 Information. In *2009 International Conference on Computer Technology and Development*. vol. 1,  
501 455–458
- 502 Liang, J., Doermann, D. S., and Li, H. (2004). Camera-based analysis of text and documents: a survey.  
503 *International Journal of Document Analysis and Recognition (IJDAR)* 7, 84–104
- 504 Magee, L. A., Von Dadelszen, P., Singer, J., Lee, T., Rey, E., Ross, S., et al. (2016). The CHIPS randomized  
505 controlled trial (control of hypertension in pregnancy study). *Hypertension* 68, 1153–1159
- 506 Mammeri, A., Khiari, E., and Boukerche, A. (2014). Road-Sign Text Recognition Architecture for  
507 Intelligent Transportation Systems. In *2014 IEEE 80th Vehicular Technology Conference (VTC2014-Fall)*.

- 510 1–5  
511 Martinez, B., Coyote, E., Hall-Clifford, R., Juarez, M., Miller, A. C., Francis, A., et al. (2018). mHealth  
512 intervention to improve the continuum of maternal and perinatal care in rural Guatemala: a pragmatic,  
513 randomized controlled feasibility trial. *Reproductive Health* 15, 120  
514 Martinez, B., Hall-Clifford, R., Coyote, E., Stroux, L., Valderrama, C. E., Aaron, C., et al. (2017). Agile  
515 development of a smartphone app for perinatal monitoring in a resource-constrained setting. *Journal of*  
516 *Health Informatics in Developing Countries* 11  
517 Matan, O., Burges, C., Lecun, Y., and Denker, J. (1995). Multi-digit recognition using a space displacement  
518 neural network 4  
519 Melchiorre, K., Sutherland, G. R., Liberati, M., and Thilaganathan, B. (2011). Preeclampsia is associated  
520 with persistent postpartum cardiovascular impairment. *Hypertension* 58, 709–715. doi:10.1161/  
521 HYPERTENSIONAHA.111.176537  
522 Microsoft (2007). Microsoft HealthVault. <https://docs.microsoft.com/en-us/healthvault/>  
523 Mishra, B., Sinha, N. D., Gidwani, H., Shukla, S. K., Kawatra, A., and Mehta, S. C. (2013). Equipment  
524 errors: A prevalent cause for fallacy in blood pressure recording-a point prevalence estimate from an  
525 Indian health university. *Indian Journal of Community Medicine* 38, 15–21  
526 Mosca, L., Benjamin, E. J., Berra, K., Bezanson, J. L., Dolor, R. J., Lloyd-Jones, D. M., et al. (2011).  
527 Effectiveness-based guidelines for the prevention of cardiovascular disease in women-2011 update: A  
528 Guideline from the American Heart Association. *Circulation* 123, 1243–1262  
529 NBC Universal News Group (2017). App Saves Lives of Maya Women  
530 In Guatemala. <https://www.nbcnews.com/globalcitizen/video/app-saves-lives-of-maya-women-in-guatemala-1039437379735>  
532 Omron Healthcare Inc (2012). Omron Healthcare BP791IT Intellisense 10 Series Plus Upper Arm BP  
533 Monitor  
534 Omron Healthcare Inc (2014). OMRON Bi-LINK Gateway  
535 Omron Healthcare Inc (2020). OMRON connect US/CAN. <https://play.google.com/store/apps/details?id=com.omronhealthcare.omronconnect>. Version = 5.7.4-06029d739  
537 Osungbade, K. O. and Ige, O. K. (2011). Public health perspectives of preeclampsia in developing countries:  
538 implication for health system strengthening. *Journal of pregnancy*  
539 Parikh, N. I., Norberg, M., Ingelsson, E., Cnattingius, S., Vasan, R. S., Domellöf, M., et al. (2017).  
540 Association of pregnancy complications and characteristics with future risk of elevated blood pressure.  
541 *Hypertension* 69, 475–483  
542 Pham, H., Dvorak, A., and Perez, M. (2018). Recognizing Call Numbers for Library Books: The Problem  
543 and Issues. In *2018 International Conference on Computational Science and Computational Intelligence*  
544 (*CSCI*). 386–391  
545 Podymow, T. and August, P. (2017). New Evidence in the Management of Chronic Hypertension in  
546 Pregnancy. *Seminars in Nephrology* 37, 398–403  
547 Powers, R. W., Roberts, J. M., Plymire, D. A., Pucci, D., Datwyler, S. A., Laird, D. M., et al. (2012). Low  
548 placental growth factor across pregnancy identifies a subset of women with preterm Preeclampsia: type 1  
549 versus type 2 preeclampsia? *Hypertension* 60, 239–246  
550 Rich-Edwards, J. W., McElrath, T. F., Karumanchi, S. A., and Seely, E. W. (2010). Breathing life into  
551 the lifecourse approach: Pregnancy history and cardiovascular disease in women. *Hypertension* 56,  
552 331–334  
553 Ruzicka, M., Akbari, A., Bruketa, E., Kayibanda, J. F., Baril, C., and Hiremath, S. (2016). How Accurate  
554 Are Home Blood Pressure Devices in Use? A Cross-Sectional Study. *PLOS ONE* 11, 1–11

- 555 Salam, R., Das, J., Ali, A., Bhaumik, S., and Lassi, Z. (2015). Diagnosis and management of preeclampsia  
556 in community settings in low and middle-income countries. *Journal of Family Medicine and Primary  
557 Care* 4, 501
- 558 Scantlebury, D. C., Schwartz, G. L., Acquah, L. A., White, W. M., Moser, M., and Garovic, V. D. (2013).  
559 The treatment of hypertension during pregnancy: When should blood pressure medications be started?  
560 *Current Cardiology Reports* 15
- 561 Scheres, L. J., Lijfering, W. M., Groenewegen, N. F., Koole, S., De Groot, C. J., Middeldorp, S., et al.  
562 (2020). Hypertensive Complications of Pregnancy and Risk of Venous Thromboembolism. *Hypertension*  
563 , 781–787
- 564 Shah, P., Karamchandani, S., Nadkar, T., Gulechha, N., Koli, K., and Lad, K. (2009). OCR-based  
565 chassis-number recognition using artificial neural networks. In *2009 IEEE International Conference on  
566 Vehicular Electronics and Safety (ICVES)*. 31–34
- 567 Smith, R. (2007). An overview of the Tesseract OCR engine. In *Ninth international conference on  
568 document analysis and recognition (ICDAR 2007)* (IEEE), vol. 2, 629–633
- 569 Stroux, L., Martinez, B., Coyote Ixen, E., King, N., Hall-Clifford, R., Rohloff, P., et al. (2016). An mHealth  
570 monitoring system for traditional birth attendant-led antenatal risk assessment in rural Guatemala.  
571 *Journal of Medical Engineering & Technology* 40, 356–371
- 572 Tesseract (2005). Tesseract GitHub repository. [https://github.com/tesseract-ocr/  
573 tesseract](https://github.com/tesseract-ocr/tesseract)
- 574 Wagner, L. K. (2004). Diagnosis and management of preeclampsia. *American family physician* 70,  
575 2317–2324
- 576 Whelton, P. K., Carey, R. M., Aronow, W. S., Casey, D. E., Collins, K. J., Himmelfarb, C. D., et al.  
577 (2018). 2017 ACC/AHA/AAPA/ABC/ACPM/AGS/APhA/ASH/ASPC/NMA/PCNA guideline for the  
578 prevention, detection, evaluation, and management of high blood pressure in adults a report of the  
579 American College of Cardiology/American Heart Association Task Force on Clinical practice guidelines.  
580 *Hypertension* 71, E13–E115
- 581 WHO (2005). The World health report: 2005: make every mother and child count
- 582 Whybrow, R., Webster, L., Girling, J., Brown, H., Wilson, H., Sandall, J., et al. (2020). Implementation of  
583 national antenatal hypertension guidelines: A multicentre multiple methods study. *BMJ Open* 10
- 584 Withings (2020). Health Mate - Total Health Tracking. [https://play.google.com/store/  
585 apps/details?id=com.withings.wiscale2](https://play.google.com/store/apps/details?id=com.withings.wiscale2)
- 586 Wu, D. D., Gao, L., Huang, O., Ullah, K., Guo, M. X., Liu, Y., et al. (2020). Increased Adverse Pregnancy  
587 Outcomes Associated with Stage 1 Hypertension in a Low-Risk Cohort: Evidence from 47 874 Cases.  
588 *Hypertension* , 772–780